



The Removal of Copper Oxides by Ethyl Alcohol Monitored *In Situ* by Spectroscopic Ellipsometry

Alessandra Satta,^{a,b,z} Denis Shamiryan,^{a,c} Mikhail R. Baklanov,^d
Caroline M. Whelan,^a Quoc Toan Le,^a Gerald P. Beyer,^a André Vantomme^b
and Karen Maex^{a,c}

^aIMEC, B-3001 Leuven, Belgium

^bInstituut voor Kern-en Stralingsfysica, Department of Physics, Katholieke Universiteit Leuven, B-3001 Leuven, Belgium

^cDepartment of Electrical Engineering, Katholieke Universiteit Leuven, B-3001 Heverlee, Belgium

^dXPEQT Limited, at IMEC, B-3001 Leuven, Belgium

As an interconnect material, copper has the disadvantage of not forming self-limiting oxides, which can negatively affect device performance and reliability. Undesired oxide layers need to be removed by *in situ* cleaning, before the copper is subjected to subsequent depositions. We have used ethyl alcohol (C_2H_5OH) as a vapor phase reducing agent to remove copper oxides formed on electroplated copper films upon exposure to the ambient. Spectroscopic ellipsometry has been used to monitor the reduction process *in situ*. *Ex situ* characterization using X-ray photoelectron spectroscopy and atomic force microscopy support *in situ* measurements. While oxide removal can be achieved at temperatures as low as 130°C, independent of oxide layer thickness and composition, it occurred more efficiently at 200°C, showing compatibility with the low temperature (<400°C) processing requirements of low dielectric constant materials. The initial reaction involves the reduction of Cu^{2+} to Cu^+ species followed by a second phase consisting of Cu^+ conversion to elemental copper, producing a clean metal surface. Reduction of Cu^{2+} to Cu^+ species is the rate-limiting step as evidenced by enhanced sensitivity to the reaction temperature.

© 2003 The Electrochemical Society. [DOI: 10.1149/1.1564108] All rights reserved.

Manuscript submitted January 25, 2002; revised manuscript received October 2, 2002. Available electronically March 20, 2003.

In order to improve the performance of interconnection systems in advanced integrated circuits, alternative conductors must be introduced to replace aluminum and its alloys.¹ Copper has been chosen for its low bulk electrical resistivity (1.7 $\mu\Omega$ cm vs. 2.7 $\mu\Omega$ cm for aluminum) and high melting point (1083 vs. 660°C for aluminum). Moreover, the electromigration resistance of copper is superior to that of aluminum, which is more susceptible to degradation and loss of electrical integrity. These properties should be of significant benefit in the effort to reduce signal transmission delays and power dissipation. In parallel, a damascene scheme accompanies the introduction of copper and replaces the reactive ion etching approach in making patterns of reduced dimensions.¹ Despite the benefits of the use of copper as interconnect metal in the damascene integration scheme, its introduction brings new challenges. One concern is related to the high diffusivity of copper in silicon, with a diffusion coefficient of about 2.0×10^{-5} cm²s⁻¹ at 500°C, which is 15 orders of magnitude higher than that of aluminum.² This behavior necessitates the use of a barrier layer to protect the active areas and the interlevel dielectrics from metal penetration. A second problem is instability to oxidation. In contrast with aluminum and its alloys, copper does not form self-passivating and stable oxide layers, resulting in poor adhesion to barrier films and adversely influencing electromigration behavior and via resistance between metal levels. Degradation of the copper interconnect is attributed to the formation of cupric oxide (CuO), that nucleates on top of cuprous oxide (Cu₂O), which typically forms in contact with metallic copper.^{3,4} In addition, exposure to ambient conditions results in the formation of copper hydroxide Cu(OH)₂^{4,5} and copper carbonate CuCO₃.^{6,7} Such contamination layers must be removed by *in situ* cleaning, before the copper is subjected to subsequent processing.

Sputter etching, previously used to remove metal oxides, has become inadequate as the dimensions of interconnect features decrease. A recent study has focused on the reduction of copper oxide to elemental copper by hydrogen plasma,⁶ which was proven efficient between 200 and 350°C. However, the major concern with this method is its compatibility with dielectric materials, such as low- k polymers, which are susceptible to damage during the cleaning pro-

cess. An alternative approach involves selective etching of copper oxides with β -diketonates,⁸⁻¹⁰ e.g., hexafluoroacetylacetone, which react almost exclusively with copper oxides to form volatile products, their high vapor pressures facilitating easy removal from the processing system. Unfortunately, the formation of Cu(I)(β -diketonate) can disproportionate into Cu(0) and Cu(I) × (β -diketonate)₂, which potentially allows copper readsorption and diffusion into the dielectric material. Nevertheless, this type of surface treatment employing gas/solid reactions has been demonstrated to be efficient at temperatures below 400°C, the maximum temperature acceptable in processing low dielectric constant materials. Processes involving selected organic compounds, containing one or more of the following functional groups: alcohol (-OH), aldehyde (-CHO), and carboxylic acid (-COOH), to reduce metal oxide layers to elemental metal have been reported.^{11,12} The influence and role of carbon and carbon-containing species in reduction reactions of copper oxides has been studied.^{13,14} Recently, Chavez and Hess have examined the ability of liquid acetic acid (CH₃COOH) to remove copper oxide layers at very low temperature (35°C).¹⁵ The authors reported the removal of a variety of copper oxides, including CuO, Cu₂O, and Cu(OH)₂ without corrosion of the underlying elemental copper film.

Similarly, our work is concerned with the selective elimination of metal oxides using organic compounds as reducing agents in an effort to develop feasible *in situ* cleaning treatments. In our study, we have used vapor phase ethyl alcohol (CH₃CH₂OH) as reducing agent. Our approach of using reducing agents in the gas phase has advantages compared to the wet chemical removal treatment in terms of enhanced flexibility and control of the cleaning process for interconnects processing applications. In this study, we have monitored the reduction of Cu oxides with ethyl alcohol using *in situ* spectroscopic ellipsometry. *Ex situ* X-ray photoelectron spectroscopy (XPS) and atomic force microscopy (AFM) analysis have provided complementary characterization.

Experimental

The evaluation of the reduction of all different copper oxide films was carried out by *in situ* spectroscopic ellipsometry. This surface analysis technique is based on the measurement of the change in the state of light polarization, defined by two quantities Δ and Ψ . From Δ and Ψ , the thickness and the refractive index of a

^z E-mail: Alessandra.Satta@imec.be

film on a substrate can be deduced.¹⁶ The experimental setup consists of a vacuum assembly designed for spectroscopic ellipsometry measurements, consisting of an ellipsometer Sentech 801, a gas handling system connecting the liquid ethyl alcohol ($\text{CH}_3\text{CH}_2\text{OH}$, Spectranal, absolute, ≥ 99.8 vol.%) reservoir and sample heating. The heating system allows temperature control within $\pm 5^\circ\text{C}$ up to a maximum of 400°C .

Electrochemically deposited (ECD) copper films were exposed to cleanroom ambient resulting in the formation of a copper oxide film, several nm in thickness. In addition, $1\ \mu\text{m}$ thick ECD films, deposited on $150\ \text{nm}$ plasma vapor-deposited (PVD) copper seed film, were intentionally oxidized by storage in an O_2 ambient at 175°C for 1 min. A thick oxide film was thus obtained. The reduction of the different copper oxide films was monitored at different sample temperatures. Once the temperature had stabilized at the predetermined setpoint (chamber pressure $\sim 5 \times 10^{-3}$ Torr), ethyl alcohol was introduced into the vacuum chamber and the copper oxide sample was exposed for a certain time period. The introduction of vapor into the chamber caused a setpoint dependent decrease in temperature (in the worst case, at 300°C , 20°C below the setpoint), due to a temperature gradient between the gas reservoir and the heater.

During the reduction of the copper oxide, performed at different temperatures, the evolution of the angles Δ and Ψ was monitored by ellipsometry measurements as a function of time. XPS measurements were performed with a SSX-100 spectrometer equipped with a monochromatic Al $\text{K}\alpha$ source. AFM measurements were carried out under ambient conditions using a Nanoscope III Dimension 3000 in tapping mode.

Results and Discussion

Ethyl alcohol reduction of native copper oxide.—To study the reduction of native oxide we have used samples of $1\ \mu\text{m}$ thick ECD copper which had been oxidized during storage in the cleanroom environment for several months. A previous study on the effect of the ambient exposure of ECD copper films has shown that the outermost layer is composed of Cu^{2+} species such as CuO and $\text{Cu}(\text{OH})_2$ with an underlying Cu^+ layer in the form of Cu_2O , in contact with elemental copper.⁴

XPS characterization of our samples reveals a shoulder on the high binding energy side of the Cu^0 peak in the $\text{Cu}\ 2\text{p}$ spectrum, shown in Fig. 1a. This peak, located at approximately $934.6\ \text{eV}$ is attributed to the presence of $\text{Cu}(\text{OH})_2$ and CuCO_3 species which cannot be distinguished.⁷ The presence of Cu^{2+} species is also reflected by the multiple component structure of the shake-up satellite between 938 and $945\ \text{eV}$.^{5,7} Figure 1b shows that the $\text{O}\ 1\text{s}$ core level region is composed of a broad asymmetric peak with a maximum at $\sim 531\ \text{eV}$. Contributions at higher binding energies ($\sim 532\ \text{eV}$) can be attributed to surface hydroxide, while CuO and Cu_2O typically give rise to peaks between 529 and $530.5\ \text{eV}$.^{3,5} It is not unusual that we also observe the presence of carbon on the samples as evidenced by $\text{C}\ 1\text{s}$ photoemission, shown in Fig. 1c. Exposure to the ambient should, in addition to oxidation, give rise to adventitious carbon contamination. The main $\text{C}\ 1\text{s}$ peak occurring at $\sim 284.7\ \text{eV}$ is characteristic of C-C and C-H type bonds. The higher binding energy component of the spectrum, located at $\sim 289\ \text{eV}$ is more informative. This feature can be assigned to the presence of species containing a carbon moiety, which is bonded to an electronegative element such as oxygen, which may conveniently be assigned to the existence of C-O bonds in CuCO_3 .^{6,7}

The reduction of the native oxide of ECD copper by ethyl alcohol was performed at temperatures ranging from 130 to 300°C . Figure 2 shows the reduction of a copper oxide film with ethyl alcohol at 200°C monitored by *in situ* ellipsometry. At fixed wavelength ($\lambda = 632.8\ \text{nm}$), the changes in the ellipsometric parameters Δ and Ψ as a function of the time provide information on the reduction process. Three phases are distinguishable in Fig. 2. In the first phase, which starts when ethyl alcohol is introduced into the chamber, the

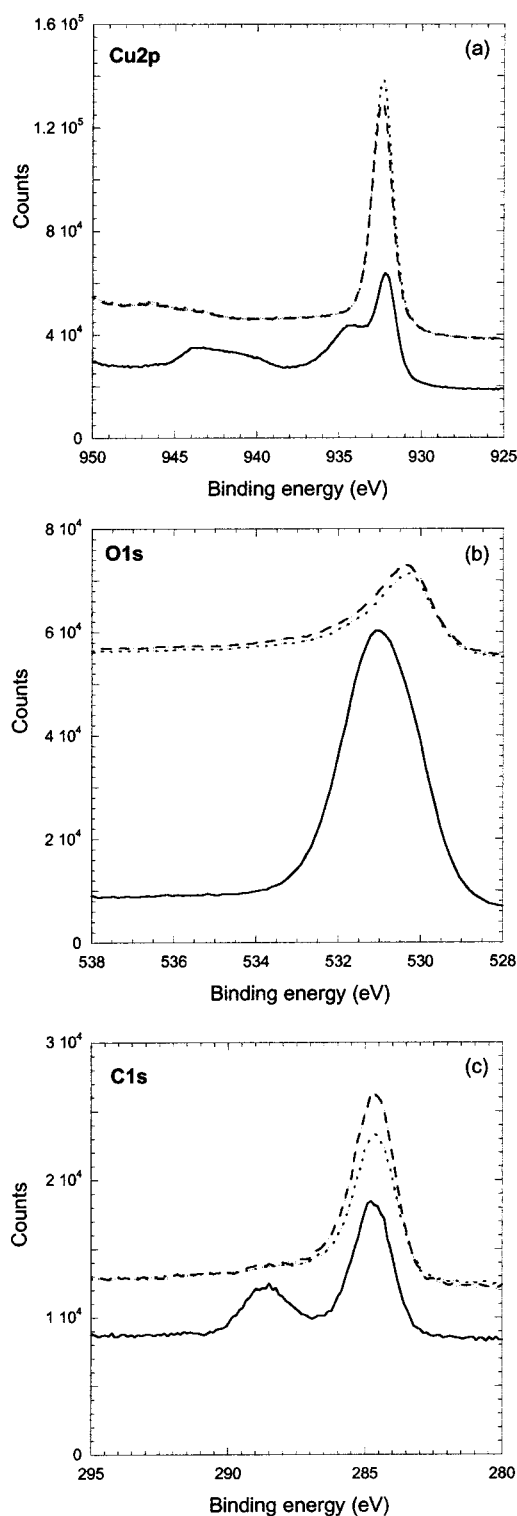


Figure 1. XPS spectra of the (a) $\text{Cu}\ 2\text{p}$, (b) $\text{O}\ 1\text{s}$, and (c) $\text{C}\ 1\text{s}$ core levels collected (—) before and after ethyl alcohol reduction of a copper oxide film at (\cdots) 200°C and (---) 300°C .

angle Δ decreases a few degrees and reaches its minimum value, about 96.3° . The angle Δ remains constant at the minimum value for a certain time, before changing to a final constant value within a few seconds, in the second phase of the curve. While Δ increases $\sim 16^\circ$, an increase of less than 1° affects the Ψ phase. The experimental error in the amplitude angle was better than 0.05° . Therefore, a small change in Ψ is significant. Constant Δ and Ψ values, repre-

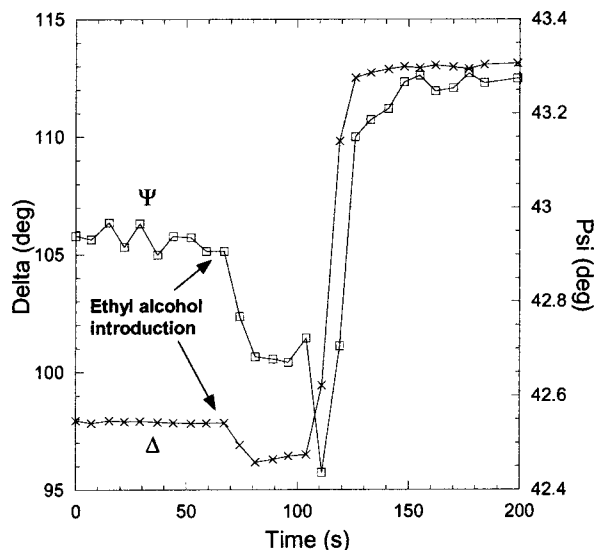


Figure 2. Changes in the ellipsometric characteristics (\times) Δ and (\square) Ψ as a function of time during ethyl alcohol reduction of a copper oxide film at 200°C.

sending the final status of the copper surface after complete reaction, characterize the third phase of the curve. The values of Δ and Ψ angles are $113.1 \pm 0.1^\circ$ and $43.2 \pm 0.1^\circ$, respectively. These angle amplitudes are close to the optical parameters obtained in the case of PVD cleaned copper surface.⁶ The reaction is therefore complete within ~ 100 s at 200°C.

In order to understand the behavior of the ellipsometric angles during the reduction reaction, model fittings of the ellipsometric data were performed. The model consists of a CuO layer on top of a Cu₂O layer in contact with metallic copper, as shown schematically in the inset in Fig. 3. It assumes that the optical constants of CuO

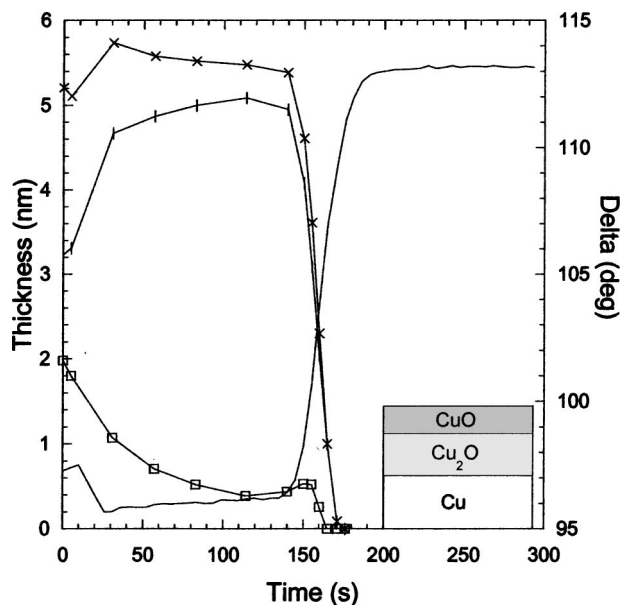


Figure 3. Variation of the of (\square) CuO and ($|$) Cu₂O and (\times) total thicknesses and the ellipsometric parameter ($—$) Δ as a function of time during ethyl alcohol reduction of a copper oxide film at 200°C. Inset: the model of oxide assumed for the simulation of spectra Δ and Ψ variations during the reduction. The optical constants of CuO and Cu₂O layers are taken from Ref. 17.

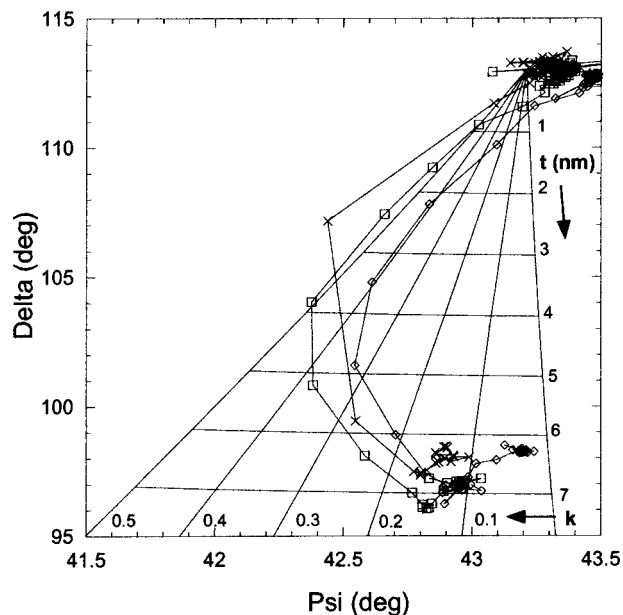


Figure 4. The evolution of Δ and Ψ during the ethyl alcohol reduction at 200°C. The network indicates a frame of reference where thickness and extinction coefficient are the new coordinates, which Δ and Ψ have to refer to.

and Cu₂O correspond to those from optically thick films, as reported in the Palik handbook of optical constants.¹⁷ The optical constants of copper, considered as the substrate, are taken as those characteristic of ECD copper cleaned by the reduction process. Since the angle of incidence was fixed at 70° , the Δ and Ψ spectra, recorded in the wavelength range of 350–850 nm, uniquely define the thickness of the two oxide layers as a function of the time, during the reduction reaction. Although optical constants of thin films can be different from those of thick films,¹⁸ calculation of thin film thickness from ellipsometry measurements using optical constants of bulk materials is reasonably accurate.

Figure 3 shows the thickness evolution of CuO and Cu₂O layers, as obtained from ellipsometry data and the variation in the Δ angle as a function of reduction reaction time. During the Δ plateau region, or first phase, the thickness of the CuO layer, calculated from the ellipsometry characteristics, decreases, while simultaneously the Cu₂O thickness increases by the same amount, but the total thickness of the oxide layer does not change. This observation indicates that the conversion of CuO to Cu₂O is the first step in the oxide removal process by ethyl alcohol reduction. A rapid thickness decrease in the Cu₂O layer, until the oxide removal is complete, occurs in the second phase of the Δ curve. After the Cu²⁺ is converted to the lower oxidation state, reduction of Cu₂O to Cu is initiated. Therefore, the second phase in the Δ and Ψ curves clearly corresponds to the complete reduction of the Cu₂O layer. Accordingly, the total thickness of the oxide drops to zero. In the third phase, when Δ and Ψ remain constant, the copper surface is reduced completely. Considering as the total process time the sum of the duration of the Δ plateau plus the duration of the rapid increase of the Δ curve, $0.38 \pm 0.10 \text{ Å s}^{-1}$ can be estimated as the overall reaction rate at 200°C for ~ 5 nm oxide film.

The slope of the Δ curve is correlated with the reduction rate. However, an accurate evaluation of the reduction rate requires an ellipsometry measurement frequency higher than the reaction rate, which is not possible in our experimental setup. The delay time between measurements of 3–4 s allows evaluation of macroscopic aspects of the reduction process but is insufficient to distinguish any microscopic details.

Figure 4 illustrates the typical evolution of Δ and Ψ amplitudes

during the ethyl alcohol reduction for several samples at 200°C. A half ellipse curve is reproduced for each sample, despite the different initial Δ and Ψ values. This half ellipse corresponds to the rapid increase in the curve observed in the Δ vs. time plot in Fig. 3, and is therefore indicative of the phase of fast reduction of Cu_2O . The network overlapping the curves in the graph represents a change of coordinates from (Δ, Ψ) to thickness and extinction coefficient (t and k , respectively). The conversion to the new coordinates requires fixing the refractive index. In this simulation, we have chosen $n=2.8$, a value close to the refractive index of the two copper oxides. In the new coordinates system, the extinction coefficient moves to high values during the initial evolution of the optical angles Δ and Ψ . The increase in the k parameter to values higher than that typical of Cu_2O ($k = 0.1$)¹⁷ during the phase of Cu_2O reduction, may indicate that the composition of the outermost layer is changing in terms of its oxygen content and therefore the formation of intermediate unstable oxide phases may take place. Moreover, embedded copper may form during the oxygen depletion in the reduction of Cu_2O , resulting in a higher extinction coefficient for the residual layer. Figure 4 also shows a simultaneous decrease in the thickness of the Cu_2O layer during the evolution of Δ and Ψ .

The *ex situ* XPS analysis of the samples shows (Fig. 1) significant changes in the Cu 2p, O 1s, and C 1s spectra following ethyl alcohol reduction of the copper samples. Components previously attributed to copper in a high oxidation state and to surface contamination with oxygen and carbon-containing species have diminished in intensity. The Cu 2p signal is now composed of a single peak located at 932.3 eV (Fig. 1a) which is the binding energy reported for elemental copper.⁷ In addition, the shoulder which had been observed on the high binding energy side of the main Cu 2p peak and the satellite structure at higher energies, associated with the presence of Cu^{2+} species, have disappeared. The significant enhancement of the Cu^0 peak intensity is also indicative of the removal of the overlaying oxide layers. In support of the Cu 2p data, the O 1s signal in Fig. 1b shows decreases in intensity and a shift to lower binding energy after the reduction reaction. The binding energy shift is due to the disappearance of the photoemission contribution associated with hydroxides. The residual O 1s peak located at ~ 530.2 eV is assigned to Cu_2O due to exposure of the samples to the ambient after the ethyl alcohol cleaning. After reduction in the ellipsometer chamber, the samples were exposed to the ambient for ~ 1 h before being introduced in the XPS vacuum chamber. During this time, a reoxidation and contamination of the clean copper samples is expected. The C 1s spectrum after reduction by ethyl alcohol (Fig. 1c) is composed of a peak at ~ 284.6 eV, also attributed to ambient contamination. The peak at higher binding energy previously assigned to the presence of C-O bonds has essentially disappeared. In conclusion, *ex situ* XPS analysis confirms that $\text{Cu}(\text{OH})_2$, CuCO_3 , and CuO are removed by ethyl alcohol treatment of oxidized ECD copper. However, due to exposure to ambient, it is not possible to draw conclusions about Cu_2O removal.

Figure 5 shows the refractive index and extinction coefficient of copper samples, before and after reduction at room temperature. The optical constants were calculated from the ellipsometric angles measured *in situ*, assuming the simple physical model of a copper substrate in contact with ambient. Neglecting the thin copper oxide layer in the model introduces some errors in the calculation of the n and k dispersions for the copper sample before reduction. Therefore, the appearance of large changes in the optical constants upon ethyl alcohol exposure indicate the removal of the oxide layer. These optical characteristics are compared with the optical constants of bulk copper, as reported in the manufacturer's database, which are based on the published data of Palik.¹⁷ The optical constants of bulk copper reduced and cleaned by ethyl alcohol. This may be due to the fact that the Palik optical constants refer to *ex situ* ellipsometric measurements¹⁷ where the copper is most likely oxidized. This explanation is supported by the position of the Palik extinction coef-

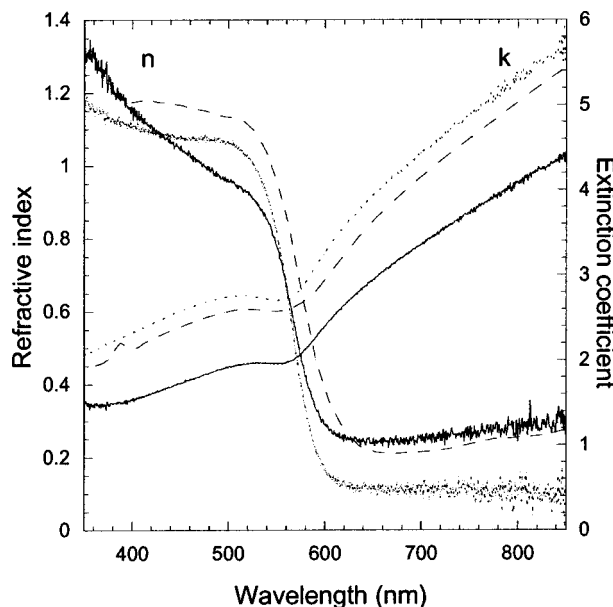
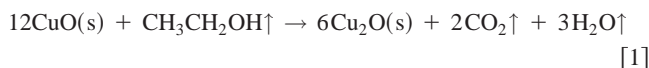


Figure 5. Refractive index and extinction coefficient dispersions for a copper film (—) before and (· · · ·) after reduction of native copper oxide with ethyl alcohol. (---) The dispersions of copper reported in Ref. 17 are shown for comparison.

ficient dispersion, which is shifted to higher values than our oxidized copper exposed to ambient conditions, but is located at lower values than the copper cleaned by ethanol and characterized *in situ*.

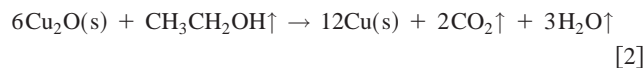
Temperature dependence of ethyl alcohol reduction of native copper oxide.—Figure 6a shows the evolution of Δ and Ψ during the ethyl alcohol reduction at different temperatures. The semi-elliptical shape of the curve, corresponding to the reduction of Cu_2O , is reproduced independent of the reaction temperature. Interestingly, at temperatures higher than 200°C, after the cleaning is completed, the Ψ angle moves toward lower values at constant Δ . This behavior may be related to changes in the microstructure of copper film at high temperature.

The evolution of Δ and Ψ during the reduction is similar at different temperatures. In a reduction/oxidation reaction, primary alcohols such as ethyl alcohol are oxidized to aldehydes, which can be further oxidized to carboxylic acids. Since aldehydes are oxidized more easily than alcohols, the oxidation of a primary alcohol is usually carried out all the way to the carboxylic acid. These compounds normally strongly resist further oxidation. However, due to the temperature enhancement of the reduction-oxidation process (in the range considered $T = 130$ – 300°C), we assume a further oxidation of the carboxylic acid, with formation of CO_2 and H_2O as byproducts of the reaction. Therefore, we assume the following balanced reactions



$$\Delta H^\circ = -95.9 \text{ kcal/mol}$$

$$\Delta S^\circ = 181.2 \text{ cal/deg mol}$$



$$\Delta H^\circ = -63.5 \text{ kcal/mol}$$

$$\Delta S^\circ = 131.4 \text{ cal/deg mol}$$

In both reactions, the copper is not removed from the surface because the formation of volatile copper compounds does not occur.

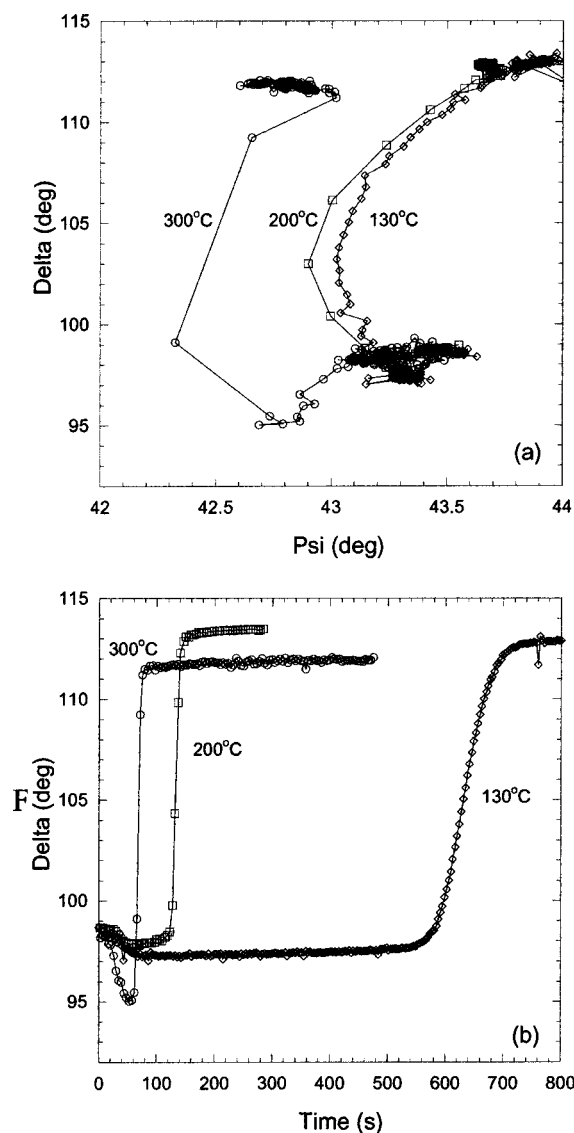


Figure 6. (a) The evolution of Δ and Ψ during ethyl alcohol reduction at (\diamond) 130°C, (\square) 200°C, and (\circ) 300°C is shown. (b) The optical parameter Δ is reported as a function of time for the different reduction temperatures. The zero point indicates the time of introduction of ethyl alcohol into the chamber.

Both the enthalpy and the entropy factors support these reactions, so that they are thermodynamically favorable at the temperatures considered, with a large release of energy during the reduction.

Figure 6b shows the Δ curves as a function of time for different process temperatures. When the temperature of reduction decreases, the reaction occurs at a slower rate. More specifically, the Δ plateau in the first stage of the reaction becomes larger as the reduction temperature decreases. This implies that the reduction of CuO to Cu_2O requires longer times at lower temperatures and constitutes the rate limiting step in the cleaning of the copper surface by ethyl alcohol. The thermodynamics of the reduction Reactions 1 and 2 indicates that the conversion from CuO to Cu_2O is energetically more favorable than the conversion of Cu_2O to Cu . Kinetic factors, such as the activation energy of the reduction $\text{CuO} \rightarrow \text{Cu}_2\text{O}$ by ethyl alcohol, may result in a slowing down of the first step in the reaction. On the other hand, other factors may contribute to inhibit the reaction as the temperature decreases. For example, the presence of contaminant layers on the copper surface could affect the kinetics of the first reduction step at low temperatures.

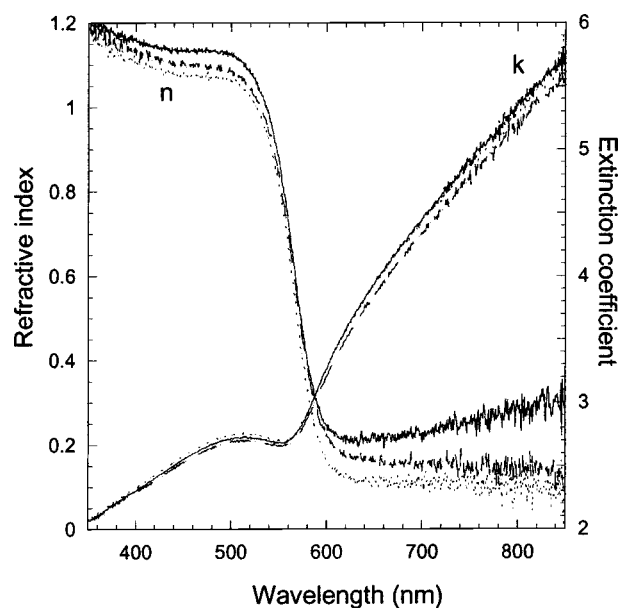


Figure 7. Refractive index and extinction coefficient dispersions for ECD copper films reduced with ethyl alcohol at 130°C (—), 200°C (· · · · ·) and 300°C (---).

The slope of the Δ curves, which correlates with the reduction rate of Cu_2O itself, also varies with temperature. A comparison between the slope of the Δ curve at 300 and 130°C, clearly indicates a different reduction rate, although the dependence on the temperature is less pronounced than in the case of the CuO reduction. This dependence clearly correlates with the activation energy of the reduction of Cu_2O to Cu .

Figure 7 shows the n and k dispersions of copper samples reduced at different temperatures and measured *in situ* at room temperature. The reduction temperature seems to affect mostly the refractive index of copper in the high wavelength region, while the extinction coefficient dispersion appears less sensitive to thermal influence.

The differences in the optical constants of the copper cleaned at different temperatures may be due to microstructural changes in the copper films. Phenomena such as recrystallization and grain growth are temperature dependent and occur readily upon annealing.^{19,20} Moreover, diffusion and segregation of impurities trapped within the ECD film is temperature dependent²⁰ and may also affect the n and k dispersions. Film surface morphology can also influence the optical constants. *Ex situ* AFM analysis reveals distinctive surface morphological changes in copper films reduced at different temperatures. Figure 8 shows a comparison of AFM images from ECD copper surface naturally oxidized and following reduction by ethyl alcohol at 200°C and 300°C. These images demonstrate that after the reduction reactions, the copper film morphology transforms such that the surface features are more peaked at 200°C, and become larger with a greater size distribution at 300°C. A comparison of XPS spectra from copper samples cleaned by ethyl alcohol at 200 and 300°C shows that the signals are almost indistinguishable (Fig. 1). Unfortunately, the composition of the surface after the reduction at different temperatures cannot be determined precisely due to recontamination of the samples upon exposure to ambient.

Reduction of thick copper oxide layers.—ECD copper samples oxidized by the ambient were further oxidized by exposure to O_2 ambient for 1 min at 175°C. Scanning electron microscope cross-sectional analysis in combination with XPS depth profile (data not shown) indicates that the so-obtained oxide is 70 nm thick and is formed by a bilayer of thick CuO and Cu_2O films. Figure 9 shows the reduction of this oxide by ethyl alcohol, as monitored by *in situ*

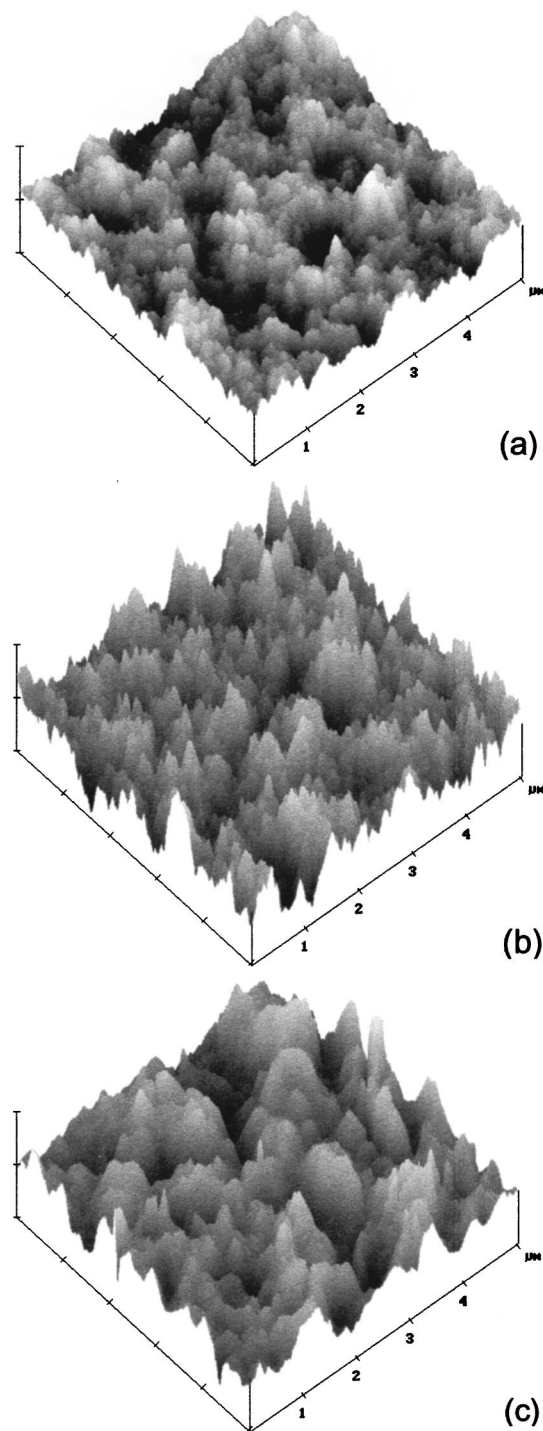


Figure 8. AFM images of ECD copper films exposed to cleanroom ambient for several months (a), and after ethyl alcohol reduction at 200°C (b) and 300°C (c).

spectroscopic ellipsometry. The final Δ and Ψ values obtained after reduction at 150 and 200°C are comparable to the ones of native oxide reduced by ethyl alcohol between 130 and 300°C. In addition, the evolution of Δ and Ψ during the reduction again follows a semi-elliptical behavior in (Δ , Ψ) space and is most likely related to a decrease in the thickness of the copper oxide films. This experiment shows that oxide removal can be achieved at low temperatures independent of oxide layer thickness and composition.

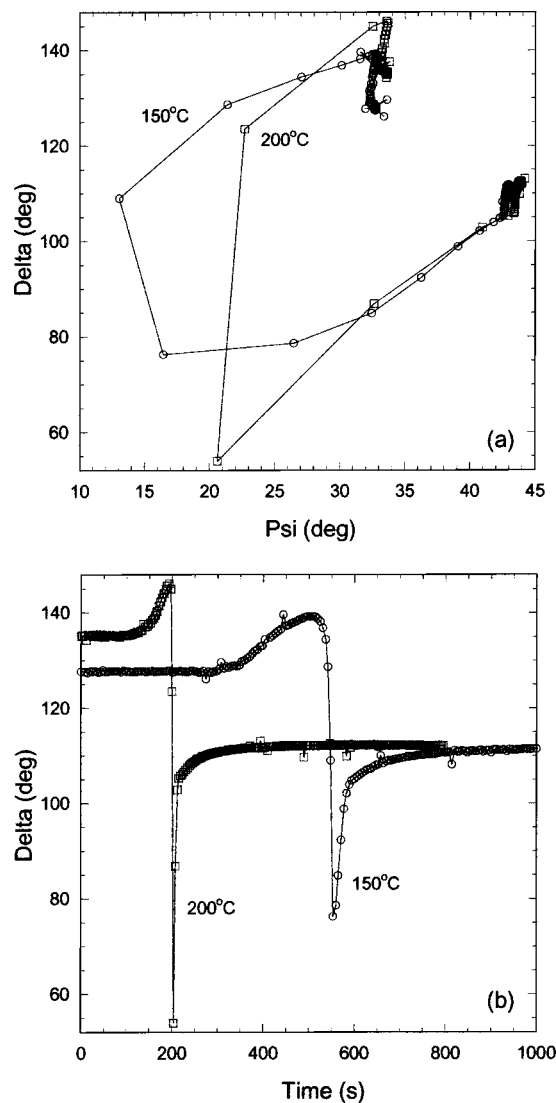


Figure 9. The evolution of Δ and Ψ (a) and the ellipsometric parameter Δ as a function of time (b) during the reduction of a 70 nm thick copper oxide film with ethyl alcohol at 150°C (○) and 200°C (□).

Conclusions

We have shown that ethyl alcohol reducing agent efficiently cleans ECD copper ambient-contaminated and thermally oxidized surfaces. Large changes in the films during the reduction process were monitored *in situ* in terms of their ellipsometric characteristics using spectroscopic ellipsometry. Such measurements were supported by *ex situ* XPS and AFM analysis. The evolution of the ellipsometric angles Δ and Ψ indicates an initial temperature sensitive step consisting of the conversion of CuO to Cu_2O . During this rate-limiting phase of the reduction reaction, the total thickness of the oxide layer remains constant. In the second phase of the reaction, which is much faster, the Cu_2O film is reduced to elemental copper. While oxide removal can be achieved at temperatures as low as 130°C, it occurred more efficiently at 200°C showing compatibility with the low temperature (below 400°C) processing requirements of low dielectric constant materials.

Acknowledgments

The authors gratefully acknowledge Ivan Callant for technical support and Laure Carbonell for the oxidation of the ECD samples.

Katholieke Universiteit Leuven and IMEC assisted in meeting the publication costs of this article.

References

1. P. Murarka, *Mater. Sci. Eng., R*, **R19**, 87 (1997).
2. A. A. Istratov and E. R. Weber, *J. Electrochem. Soc.*, **149**, G21 (2002).
3. F. M. Pan, S. R. Horng, T. D. Yang, and V. Tang, *J. Vac. Sci. Technol. A*, **8**, 4074 (1990).
4. E. Apen, B. R. Rogersand, and J. A. Sellers, *J. Vac. Sci. Technol. A*, **16**, 1227 (1998).
5. S. Poulston, P. M. Parlett, P. Stone, and M. Bowker, *Surf. Interface Anal.*, **24**, 811 (1996).
6. M. R. Baklanov, D. G. Shamirian, Zs. Tökei, G. P. Beyer, T. Conard, S. Vanhaelemeersch, and K. Maex, *J. Vac. Sci. Technol. B*, **19**, 1201 (2001).
7. P. J. Matsuo, T. E. F. M. Standaert, S. D. Allen, and G. S. Oehrlein, *J. Vac. Sci. Technol. B*, **17**, 1435 (1999).
8. T. Nguyen, L. J. Charneski, D. R. Evans, and S. T. Hsu, U.S. Pat. 5,939,334 (1999).
9. A. Sekiguchi, A. Kobayashi, T. Koide, O. Okada, and N. Hosokawa, *Jpn. J. Appl. Phys., Part 1*, **39**, 6478 (2000).
10. S.-W. Kang, H.-U. Kim, and S.-W. Rhee, *J. Vac. Sci. Technol. B*, **17**, 154 (1999).
11. P. J. Soininen, K.-E. Elers, PCT Pat. Application WO0188972 (2001).
12. P. J. Soininen and K.-E. Elers, abstracts in *Proceedings of the Advanced Metallization Conference (AMC)*, Oct. 2001, Montreal, Canada.
13. J. Li, G. Vizkelethy, P. Revesz, J. W. Mayer, L. J. Matienzo, F. Emmi, C. Ortega, and J. Siejka, *Appl. Phys. Lett.*, **58**, 1344 (1991).
14. R. Schubert, *Phys. Rev. B*, **43**, 1433 (1991).
15. K. L. Chavez and D. W. Hess, *J. Electrochem. Soc.*, **148**, G640 (2001).
16. R. M. A. Azzam, N. M. Bashara, in *Ellipsometry and Polarized Light*, Chap. 4, p. 269, North Holland, Amsterdam (1977).
17. *Handbook of Optical Constants of Solids II*, E. D. Palik, Editor, Academic Press, New York (1991).
18. C. Liu, J. Erdmann, J. Maj, and A. Macrander, *J. Vac. Sci. Technol. A*, **17**, 2741 (1999).
19. C. H. Seah, S. Mrida, and L. H. Chan, *J. Vac. Sci. Technol. A*, **17**, 1963 (1999).
20. S. Brongersma, E. Kerr, I. Vervoort, A. Saerens, and K. Maex, *J. Mater. Res.*, **17**, 582 (2002).